

Optimal H_∞ Control for Linear Periodically Time-Varying Systems in Hard Disk Drives

Jianbin Nie, Richard Conway, and Roberto Horowitz

Computer Mechanics Laboratory
Mechanical Engineering
University of California, Berkeley, CA, USA

January 2, 2012

Abstract

Periodicity frequently occurs in hard disk drives (HDDs) whose servo systems with periodic phenomena can be usually modeled as linear periodically time-varying (LPTV) systems. This paper discusses optimal H_∞ control synthesis for discrete-time LPTV systems via discrete Riccati equations. First, an explicit minimum entropy H_∞ controller for general time-varying systems is obtained. Subsequently, the developed control synthesis algorithm is applied to LPTV systems and it is shown that the resulting controllers are periodic. The proposed control synthesis technique is evaluated through both single-rate and multi-rate optimal H_∞ track-following control designs. The single-rate servo design shows that our proposed control synthesis technique is more numerically robust in calculating optimal H_∞ controllers for discrete-time linear time-invariant systems than the Matlab function of “hinfsyn”, while the multi-rate servo design validates its ability of synthesizing multi-rate controllers to achieve the robust performance of a desired error rejection function. Moreover, an experimental study—in which the developed control synthesis algorithm on a real HDD with missing position error signal sampling data is implemented—further demonstrates its effectiveness in handling LPTV systems with a large period and attaining desirable disturbance attenuation.

1 Introduction

Linear periodically time-varying systems (LPTV) are frequently encountered in mechatronic systems [1] including hard disk drives (HDDs), in which the rotation of the disks induces periodic dynamic phenomena. For example, HDD servos with missing position error signal (PES) sampling data has been modeled as LPTV systems according to their natural periodicity related to the disk rotation [2]. Moreover, as illustrated in this paper, HDD servo systems with multi-rate sampling and actuation [3] can be easily represented as LPTV systems for control synthesis purposes. In this paper, the control design of LPTV systems in HDDs will be considered.

Since there tend to be large variations in HDD dynamics [4] due to variations in manufacture and assembly, the synthesized controller must guarantee the desired level of performance for a large set of HDDs. H_∞ control is a popular control design methodology to make control systems achieve the robust performance criterion that many several HDDs simultaneously satisfy a desired minimum level of error rejection loop shaping [5]. These techniques are potentially attractive in the design of mass-market mechatronic devices, especially HDDs, where consistent performance must be attained among tens of thousands of units in a given product line [6]. Furthermore, as shown in this paper, it is useful to extend these optimal H_∞ control design techniques to LPTV systems in HDD servos.

Since the pioneering work of Zames in [7], significant progress has been made in the design of optimal H_∞ control. In [8], a state-space solution to standard H_∞ control problems was given for continuous-time linear time-invariant (LTI) systems. As stated in [9], even though H_∞ control problems for discrete-time LTI systems can be solved by using the well-known bilinear transformation, it is more beneficial to solve the problems directly in the discrete-time domain. Peters and Iglesias [10] considered H_∞ control synthesis techniques for discrete-time linear time-varying systems via the minimum-entropy control paradigm. Using the results and ideas presented in [10], we derive explicit and implementable solutions for optimal H_∞ control of LPTV systems. These solutions via discrete Riccati equations are often more computationally efficient and accurate than the counterpart using semi-definite programs (SDP) [11].

In order to evaluate the effectiveness of the developed optimal H_∞ control synthesis algorithm, we first consider the optimal H_∞ track-following servo design for HDD servo systems with both single-rate and multi-rate sampling and actuation. The single-rate servo design shows that our proposed control synthesis technique is more numerically robust in calculating optimal H_∞ controllers for discrete-time LTI systems than the Matlab function “hinfyn”, while the multi-rate servo design validates its ability of synthesizing multi-rate controllers to achieve robust performance in terms of a desired error rejection function. Additionally, an experimental study, carried out on a real disk drive with missing PES sampling data, demonstrates that the proposed control synthesis algorithm is also applicable to LPTV systems with a large period.

This paper is organized as follows: Section 2 provides preliminary background for the results contained in the paper. In Section 3, the optimal H_∞ control synthesis algorithm for LPTV systems is explicitly determined. The

developed control methodology is applied to design H_∞ track-following controllers in Section 4. An experimental study is provided in Section 5. Conclusions are given in Section 6.

2 Preliminaries

Here, we will consider general discrete-time linear periodically time-varying systems that admit a state-space realization with periodically time-varying entries of the form

$$G \sim \begin{bmatrix} x(k+1) \\ z(k) \\ y(k) \end{bmatrix} = \left[\begin{array}{c|cc} A(k) & B_1(k) & B_2(k) \\ \hline C_1(k) & D_{11}(k) & D_{12}(k) \\ C_2(k) & D_{21}(k) & 0 \end{array} \right] \begin{bmatrix} x(k) \\ w(k) \\ u(k) \end{bmatrix} \quad (1)$$

where $w(k)$ and $u(k)$ are respectively the disturbance and control inputs; $y(k)$ is the measurable output which is accessible to the control system; $z(k)$ is ‘‘performance monitoring’’ output, used in our optimization cost function. All time-varying matrix entries in G are assumed to be periodic with period N , e.g. $A(k) = A(k+N)$.

Throughout this paper, we will use the following notations, $B(k) = \begin{bmatrix} B_1(k) & B_2(k) \end{bmatrix}$, $D_{1\bullet}(k) = \begin{bmatrix} D_{11}(k) & D_{12}(k) \end{bmatrix}$, $C(k) = \begin{bmatrix} C_1(k) \\ C_2(k) \end{bmatrix}$, $D_{\bullet 1}(k) = \begin{bmatrix} D_{11}(k) \\ D_{21}(k) \end{bmatrix}$, and $D(k) = \begin{bmatrix} D_{11}(k) & D_{12}(k) \\ D_{21}(k) & 0 \end{bmatrix}$.

Before providing our developed control algorithm for the LPTV system in (1), we have the following notations and assumptions similar to the counterpart in [10]. The input disturbance $w(k)$ is assumed to belong to ℓ_2 , the set of all square summable sequences. In addition, the H_∞ norm of linear time-invariant systems is generalized as the ℓ_2 induced norm for discrete-time linear time-varying (LTV) systems. For an LTV system H with input w and output z , its ℓ_2 induced norm is defined as

$$\|H\|_{2 \leftarrow 2} = \left(\sup_{w \in \ell_2 \setminus \{0\}} \frac{\sum_{k=0}^{\infty} z^T(k)z(k)}{\sum_{k=0}^{\infty} w^T(k)w(k)} \right)^{1/2}.$$

A bold operator will denote a linear operator corresponding to a time-varying system. For example, if \mathbf{H} is the linear operator corresponding the time-varying system H , \mathbf{H} has the matrix representation

$$\mathbf{H} = \begin{bmatrix} \ddots & \vdots & \vdots & \ddots \\ \cdots & H_{0,0} & H_{0,1} & \cdots \\ \cdots & H_{1,0} & H_{1,1} & \cdots \\ \ddots & \vdots & \vdots & \ddots \end{bmatrix}. \quad (2)$$

Suppose now that, the LTV system H in (2) satisfies $\|H\|_{2\leftarrow 2} < \gamma$. Then, the self-adjoint operator $I - \gamma^{-2}H^*H$ has the spectral factorization

$$I - \gamma^{-2}H^*H = M^*M$$

where M is a memoryless operator. The entropy of the LTV system H [10] is defined as

$$E(H, \gamma) := -\gamma^2 \text{diag} \left\{ \ln \det(M_{k,k}^T M_{k,k}) \right\}_{k=0}^{\infty}. \quad (3)$$

Given the LPTV system defined in (1), the optimal H_∞ control objective is to find a minimum $\gamma > 0$ and an optimal linear time-varying compensator K with input $y(k)$ and output $u(k)$ so that the ℓ_2 induced norm of the closed-loop system $\mathcal{F}_\ell(G, K)$ that represents the closed-loop system with the input $w(k)$ and the output $z(k)$ as depicted in Fig. 1, is less than γ , i.e.

$$\begin{aligned} \min_{K, \gamma} \quad & \gamma \\ \text{s.t.} \quad & \|\mathcal{F}_\ell(G, K)\|_{2\leftarrow 2} < \gamma. \end{aligned} \quad (4)$$

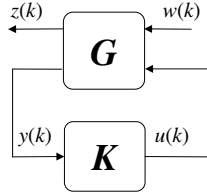


Figure 1: Block diagram of general LPTV control systems

3 H_∞ Control Synthesis for Discrete-Time LPTV Systems

As mentioned in [10], there may exist many controllers that satisfy the inequality in (4) for a given γ . Using the minimum entropy control framework allows us to choose one particular controller that satisfies the inequality in (4) for given γ . The usefulness of this framework is that the optimal controller can be synthesized using two Riccati equations. Also, the closed-loop entropy can be used to determine a bound on the closed-loop H_2 norm, which means that minimum entropy controllers tend to yield systems with small closed-loop H_2 norms. Note that the entropy for a time-varying system in (3) is defined as a memoryless operator. Unlike the minimum entropy for an LTI system, the minimum entropy for an LTV system means that its average entropy is minimum.

In order to synthesize the optimal H_∞ controller, we first need to check whether or not there exists a controller satisfying the ℓ_2 induced norm constraint in (4) for each γ , and then utilize a bi-section search method to find the

minimum γ and the corresponding optimal controller. In the minimum entropy control synthesis methodology that follows, for simplicity and without loss of generality, we will assume that $\gamma = 1$.

3.1 Minimum Entropy Control for General Discrete-Time LTV Systems

In this subsection, we will temporarily ignore the periodicity of the LPTV system in (1) and utilize the similar techniques presented in [10] to synthesize the minimum entropy output-feedback control for general linear time-varying systems. In [10], the solution to the output feedback control problem is obtained by transforming the output feedback control problem to an output estimation control problem and then using duality to transform this problem into a disturbance feedforward control problem, which is solved using the solution of a full information control problem. However, no explicit formulae are presented in [10] for controllers synthesized using these steps. Alternatively, this paper synthesizes the output feedback minimum entropy control for general discrete-time LTV systems in the following three steps:

- (I) The output feedback control problem is transformed to an output estimation control problem.
- (II) The output estimation control problem is reduced to the full control problem.
- (III) The solution to the full control problem is obtained as the dual of the full information control problem, whose solution is provided in [10].

The details of the proposed techniques for the output feedback control problem reduction is presented in [12]. Utilizing our proposed procedure yields the following unique stabilizing minimum entropy time-varying controller K which satisfies the constraint in (4) and is given by the following state space realization:

$$\begin{cases} \hat{x}(k+1) = \bar{A}(k)\hat{x}(k) + B_2(k)u(k) + F_r(k) (\bar{C}_2(k)\hat{x}(k) - y(k)) \\ u(k) = -T_{22}^{-1}(k)\bar{C}_{12}(k)\hat{x}(k) + L_r(k) (\bar{C}_2(k)\hat{x}(k) - y(k)) \end{cases} \quad (5)$$

The parameters used to construct the controller in (5) are updated in the following steps:

- 1) Solve backwards in time the state feedback Riccati equation for all j :

$$X(j) = A^T(j)X(j+1)A(j) + C_1^T(j)C_1(j) - M(j) \times (R(j) + B^T(j)X(j+1)B(j))^{-1} M^T(j) \quad (6)$$

where $M(j) = A^T(j)X(j)B(j) + C_1^T(j)D_{1\bullet}(j)$ and $R(j) = D_{1\bullet}^T(j)D_{1\bullet}(j) - \begin{bmatrix} I & 0 \\ 0 & 0 \end{bmatrix}$, so that the solution $X(j) (\geq 0)$ is bounded for all j .

After obtaining the solution $X(j)$ for all $j = 0, 1, 2, \dots$, we continue to calculate the other parameters.

2) Define $T(k) = \begin{bmatrix} T_{11}(k) & 0 \\ T_{21}(k) & T_{22}(k) \end{bmatrix}$ with $T_{11}(k) \succ 0$ and $T_{22}(k) \succ 0$, and compute $T(k)$ using:

$$R(k) + B^T(k)X(k+1)B(k) = T^T(k)JT(k) \quad (7)$$

$$\text{where } R(k) = D_{1\bullet}^T(k)D_{1\bullet}(k) - \begin{bmatrix} I & 0 \\ 0 & 0 \end{bmatrix}, J = \begin{bmatrix} -I & 0 \\ 0 & I \end{bmatrix}.$$

3) Get $\begin{bmatrix} F_1(k) \\ F_2(k) \end{bmatrix} = (R(k) + B^T(k)X(k+1)B(k))^{-1} M^T(k)$.

4) Calculate the following matrices for the filtering Riccati equation: $\bar{A}(k) = A(k) + B_1(k)F_1(k)$, $\bar{C}_2(k) = C_2(k) + D_{21}(k)F_1(k)$, and $\bar{C}_{12}(k) = -T_{22}(k)F_2(k)$. Let $D_{\perp}(k)$ be an orthogonal matrix of $D_{12}(k)$. In addition, define a matrix W such that $W^T(k)W(k) = I - T_{11}^T(k)T_{11}(k)$ and $W(k)$ has appropriate dimensions so that the following matrix multiplication is well defined:

$$\begin{bmatrix} \bar{D}_{111}(k) \\ \bar{D}_{112}(k) \end{bmatrix} = D_{\perp}(k)W(k) + D_{12}(k)T_{21}(k)$$

5) Update forwards in time the filtering Riccati equation solution with zero initial condition:

$$Y(k) = \bar{A}(k)Y(k-1)\bar{A}^T(k) + B_1(k)B_1^T(k) - \tilde{M}(k) \times \left(\tilde{R}(k) + \begin{bmatrix} \bar{C}_{12}(k) \\ \bar{C}_2(k) \end{bmatrix} Y(k-1) \begin{bmatrix} \bar{C}_{12}(k) \\ \bar{C}_2(k) \end{bmatrix}^T \right)^{-1} \tilde{M}^T(k) \quad (8)$$

where $Y(k) \succeq 0$ and

$$\begin{aligned} \tilde{M}(k) &= \bar{A}(k)Y(k-1) \begin{bmatrix} \bar{C}_{12}(k) \\ \bar{C}_2(k) \end{bmatrix}^T + B_1(k) \begin{bmatrix} \bar{D}_{112}(k) \\ D_{21}(k) \end{bmatrix}^T \\ \tilde{R}(k) &= \begin{bmatrix} \bar{D}_{112}(k) \\ D_{21}(k) \end{bmatrix} \begin{bmatrix} \bar{D}_{112}(k) \\ D_{21}(k) \end{bmatrix}^T - \begin{bmatrix} I & 0 \\ 0 & 0 \end{bmatrix}. \end{aligned}$$

6) Define $\tilde{T}(k) = \begin{bmatrix} \tilde{T}_{11}(k) & \tilde{T}_{12}(k) \\ 0 & \tilde{T}_{22}(k) \end{bmatrix}$, with $\tilde{T}_{11}(k) \succ 0$ and $\tilde{T}_{22}(k) \succ 0$, and compute $\tilde{T}(k)$ using

$$\tilde{R}(k) + \begin{bmatrix} \tilde{C}_{12}(k) \\ \tilde{C}_2(k) \end{bmatrix} Y(k-1) \begin{bmatrix} \tilde{C}_{12}(k) \\ \tilde{C}_2(k) \end{bmatrix}^T = \tilde{T}(k) \tilde{J} \tilde{T}^T(k) \quad (9)$$

where $\tilde{J} = \begin{bmatrix} -I & 0 \\ 0 & I \end{bmatrix}$.

7) Obtain

$$\begin{bmatrix} \tilde{F}_1(k) \\ \tilde{F}_2(k) \end{bmatrix} = \left(\tilde{R}(k) + \begin{bmatrix} \tilde{C}_{12}(k) \\ \tilde{C}_2(k) \end{bmatrix} Y(k-1) \begin{bmatrix} \tilde{C}_{12}(k) \\ \tilde{C}_2(k) \end{bmatrix}^T \right)^{-1} \tilde{M}^T(k). \quad (10)$$

8) Calculate the filter gains:

$$\begin{aligned} L_i(k) &= T_{22}^{-1}(k) \tilde{T}_{12}(k) \tilde{T}_{22}^{-1}(k), \\ F_i(k) &= \tilde{F}_1^T(k) \tilde{T}_{12}(k) \tilde{T}_{22}^{-1}(k) + \tilde{F}_2^T(k). \end{aligned}$$

3.2 H_∞ Control Synthesis Algorithm for LPTV Systems

It should be noted that, because we are solving an infinite horizon problem and the state feedback Riccati equation given in Step 1) must be solved backwards in time, there is no methodology for determining the solution in general [10]. Thus, the controller in (5) is not implementable for general time-varying systems. However, it is well known that the bounded stabilizing solutions to the Riccati equations in Step 1) and Step 5) are unique [10]. Moreover, we will show in Lemma 1, these solutions for LPTV systems are also periodic. As a result, the solutions to two Riccati equations converge to the corresponding stabilizing solutions, which can be solved in a straightforward manner by iteration, starting respectively from zero final and initial conditions.

Lemma 1. *For LPTV systems with period N , the solutions to the Riccati equations in both Step 1) and Step 5) are periodic with period N . Furthermore, the H_∞ controller given by (5) is also periodic with period N .*

Proof

First, we will show the periodicity of the solution to the discrete Riccati equation (6) in Step 1). Suppose $(\dots, X(j), X(j+1), \dots)$

is a solution to the discrete Riccati equation in (6), which means that

$$X(j) = A^T(j)X(j+1)A(j) + C_1^T(j)C_1(j) - \eta_j(X(j+1))$$

where

$$\begin{aligned} \eta_j(X(j+1)) = & M_j(X(j+1)) (R(j) + B^T(j) \times \\ & X(j+1)B(j))^{-1} M_j^T(X(j+1)) \end{aligned}$$

and

$$M_j(X(j+1)) = A^T(j)X(j+1)B(j) + C_1^T(j)D_{1\bullet}(j).$$

Then, at the time of $j+N$, we have

$$\begin{aligned} X(j+N) = & A^T(j+N)X(j+N+1)A(j+N) + \\ & C_1^T(j+N)C_1(j+N) - \eta_{j+N}(X(j+N+1)). \end{aligned}$$

By considering that the plant G in (1) is periodic with period N (i.e. $A(j+N) = A(j)$, $B(j+N) = B(j)$, $C_1(j+N) = C_1(j)$, and $D_{1\bullet}(j+N) = D_{1\bullet}(j)$), we have:

$$\begin{aligned} X(j+N) = & A^T(j)X(j+N+1)A(j) + \\ & C_1^T(j)C_1(j) - \eta_j(X(j+N+1)) \end{aligned} \quad (11)$$

where

$$\begin{aligned} \eta_j(X(j+N+1)) = & M_j(X(j+N+1)) (R(j) + B^T(j) \times \\ & X(j+N+1)B(j))^{-1} M_j^T(X(j+N+1)). \end{aligned}$$

Thus, the equation in (11) implies that $(\dots, X(j+N), X(j+N+1), \dots)$ is another solution to the discrete Riccati equation in (6). From [10], we know that the bounded stabilizing solution to the discrete Riccati equation in (6) is unique, which implies $X(j) = X(j+N)$.

As a result, all matrices $\bar{A}(k)$, $\begin{bmatrix} \bar{C}_{12}(k) \\ \bar{C}_2(k) \end{bmatrix}$, and $\begin{bmatrix} \bar{D}_{112}(k) \\ D_{21}(k) \end{bmatrix}$ for (8) are periodic with period N .

Moreover, the periodicity of the solution to the discrete Riccati equation (8) in Step 5), i.e. $Y(k) = Y(k + N)$, can be shown in a similar manner. Consequentially, the periodicity of $X(k)$ and $Y(k)$ implies that all of the parameters to construct the H_∞ controller in (5) are periodic with period N . Thus, the optimal H_∞ controller for the linear periodically time-varying system G is also periodic with period N .

The periodicity of H_∞ controllers for LPTV systems provides a significant advantage, since the Riccati equations in Step 1) and Step 5) can be solved backward and forward respectively with zero initial conditions by iteration and their solutions will converge to the corresponding periodic solutions.

With Lemma 1, the optimal H_∞ control synthesis algorithm for LPTV systems is developed as follows.

Algorithm 1. *The following algorithm synthesizes optimal H_∞ control for general LPTV systems.*

S1. *Choose a large initial interval and a large initial value γ .*

S2. *For a given value γ , calculate the minimum entropy controller:*

- *Solve the state feedback Riccati equation (6) in Step 1) with zero final conditions by iteration to obtain $X(j)$ ($j = 0, \dots, N - 1$).*
- *If $X(j) \succeq 0$ and the factorization in (7) exists for $\forall j = 0, \dots, N - 1$, continue to solve the filtering Riccati equation in (8) with zero initial conditions by iteration to obtain $Y(k)$ ($k = 0, \dots, N - 1$). Otherwise, stop.*
- *If $Y(k) \succeq 0$ and the factorization in (9) exists for $\forall k = 0, \dots, N - 1$, continue to calculate the control parameters for the minimum entropy controller. Otherwise, stop.*

S3. *If the interval is small enough, stop. Otherwise, update the interval and γ and then go back to S2.*

4 Design Examples for HDD Servo Systems

In order to evaluate our proposed optimal H_∞ control design methodology in this paper, the algorithm will first be tested via a simulation study that utilizes a single-stage HDD benchmark model developed by the IEEJapan technical committee on Nano-Scale Servo (NSS) systems [13]. The nominal voice coil motor (VCM) model is indicated in Fig. 2. In the simulations, we will assume that the PES sampling frequency is $f_s = 26400$ Hz.

Notice that in this paper, we consider the real VCM plant with an output multiplicative uncertainty as

$$G_v = G_v^n(1 + W_\Delta \Delta), \|\Delta\|_\infty < 1 \quad (12)$$

where W_Δ is plant uncertainty weighting function.

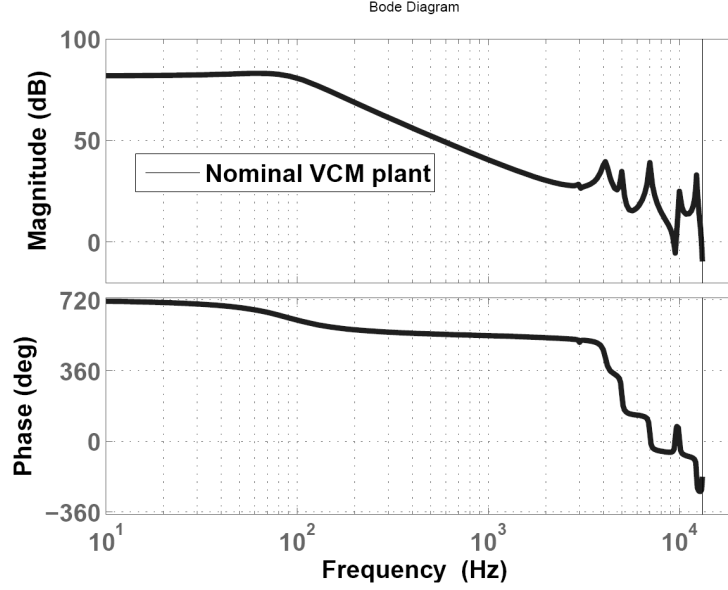


Figure 2: HDD benchmark VCM model

4.1 Optimal H_∞ Track-Following Control for Single-Rate HDD Servos

We consider the block diagram shown in Fig. 3 for the optimal H_∞ control design, where G_v^n , W_p , and W_u are respectively the nominal VCM plant, loop-shaping performance weighting function, and control input weighting value. In this example, we consider the case when the control actuation is performed at the same rate as the PES sampling rate. Thus, it is well known that the single-rate servo system is an LTI system, which is equivalent to an LPTV system with

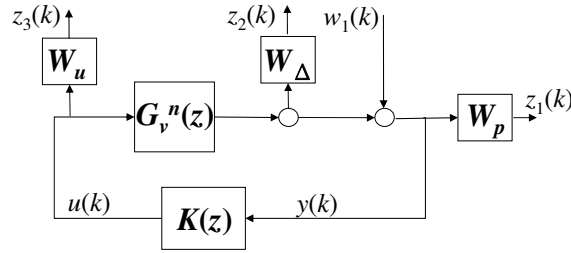


Figure 3: Control design formulation for single-rate HDDs

period $N = 1$. As a result, the corresponding control problem can be equivalently stated as:

$$\begin{aligned} \min_{K, \gamma} \quad & \gamma \\ \text{s.t.} \quad & \|T_{z \leftarrow w_1}\|_\infty < \gamma. \end{aligned} \quad (13)$$

$T_{z \leftarrow w_1}$ represents the transfer function matrix from w_1 to $z = \begin{bmatrix} z_1 & z_2 & z_3 \end{bmatrix}^T$ as shown in Fig. 3.

Notice that with $N = 1$, all of entries in the state-space realization of (1) are constant, and thus the Riccati equation

solutions in (6) and (8) converge to constant steady-state solutions that can be computed via their corresponding discrete algebraic Riccati equations (DAREs). Consequentially, the synthesized optimal H_∞ controllers for LTI systems are also time-invariant.

In order to investigate the accuracy of the control synthesis algorithm presented in this paper, we compare a controller that is synthesized by Algorithm 1 to the one that is synthesized by the Matlab function of “hinfsyn” in the Robust Control Toolbox using identical plant parameters and weighting functions. Notice that “hinfsyn” function in the Matlab version of R2007b performs H_∞ control synthesis for discrete-time systems by first mapping the discrete-time plant to a continuous-time plant using the bilinear transformation, performing H_∞ control synthesis in continuous-time domain and then mapping the resulting H_∞ continuous-time control back to discrete-time domain using the bilinear transformation.

For the comparison, the weighting functions W_p and W_Δ and the weighting value W_u are selected so that the developed H_∞ control synthesis technique yields a solution to the minimization problem in (13) with $\gamma \leq 1$. In this paper, the continuous-time uncertainty weighting function is chosen as

$$W_\Delta(s) = \frac{0.11s + 767.8}{s + 9598}. \quad (14)$$

In this section, $W_u = 2 \times 10^{-5}$ was selected so that the achieved γ is less than or equal to 1 and simultaneously the control actuation generated by the resulting controller is appropriate under the hardware constraints of real HDD servo systems.

For the single-rate design, the magnitude Bode plot of the performance weighting function inverse is illustrated in Fig. 4. With $\gamma \leq 1$, the designed servo is able to achieve the robust performance that the magnitude Bode plot of the designed error rejection transfer function is below that of $|W_p(\omega)|^{-1}$ for all uncertainties characterized by the uncertainty weighting function W_Δ in (14).

The design results are illustrated in Fig. 5, which shows the magnitude Bode plot of the closed-loop error rejection transfer functions when the H_∞ controller is synthesized using the methodology proposed in this paper and when it is synthesized using the Matlab function “hinfsyn”. As shown in the figure, the Matlab function “hinfsyn” failed to synthesize a controller that could achieve the specified robust performance, while the synthesis technique proposed in this paper produced an optimal H_∞ controller that satisfied all constraints with a minimum $\gamma^* = 0.99$. As stated in [9], the successive uses of the bilinear transformation (discrete time to continuous time and then back to discrete time) in the Matlab function “hinfsyn” may introduce numeric accuracy problems, particularly when the systems are ill-conditioned.

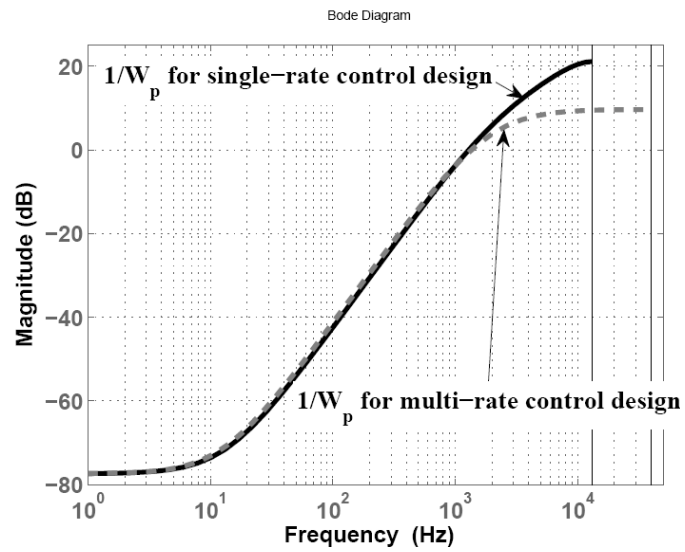


Figure 4: Magnitude Bode plots of performance weighting functions

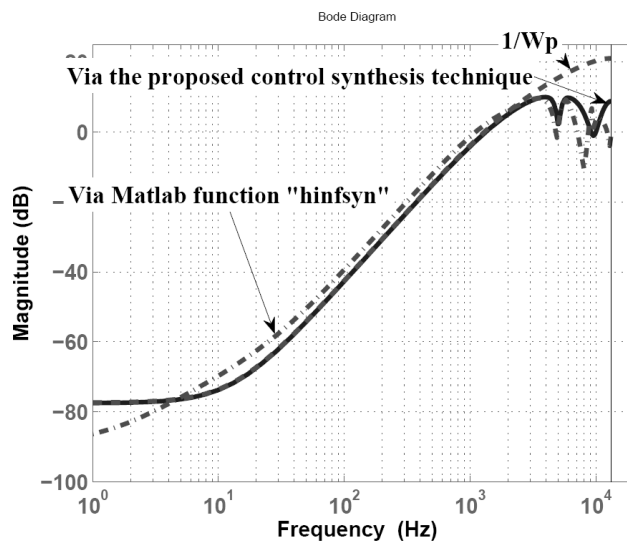


Figure 5: Sensitivity functions for the single-rate HDD servo

4.2 Optimal H_∞ Track-Following Control for Multi-Rate HDD Servos

In this subsection, the effectiveness of the developed control synthesis algorithm will be evaluated by designing optimal H_∞ track-following controllers for multi-rate HDD servos. As discussed in [14, 15], increasing the control actuation rate can improve both track-following control performance and robustness. In this subsection, we validate this idea by comparing the single-rate H_∞ controller that was designed in the previous section to a multi-rate H_∞ controller, where the actuation rate f_a is three times higher than the PES sampling rate f_s . In addition, since the higher rate actuation can be exploited to improve the control performance, a more aggressive performance weighting function, shown in Fig. 4, has been utilized for the multi-rate control design. Because of the higher actuation rate, it is necessary to discretize the plant model and the weighting functions indicated in Fig. 3 at the actuation rate f_a , i.e. at the faster rate. We then assume that PES measurements are only available at the instances $k \in \{0, N, 2N, \dots\}$ where $N = 3$. Thus, HDD servo control systems with multi-rate sampling and actuation can be modeled by the block diagram shown in Fig. 6. Here, d is the overall contribution of all disturbances [16] including torque disturbance, windage, non-repeatable disk

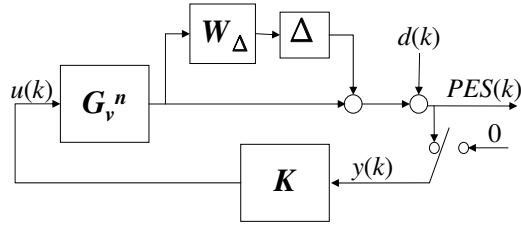


Figure 6: The HDD servo system with unavailable PES samples

motions and measurement noise to PES. For the optimal H_∞ control of such a multi-rate HDD servo system, we are also interested in designing a controller K satisfying the following conditions:

$$\|T_s \cdot W_p\|_{2 \leftarrow 2} < 1, \forall \|\Delta\|_\infty \leq 1 \quad (15)$$

where T_s is the sensitivity function (i.e. error rejection transfer function) from d to PES , as shown in Fig. 6, while W_p is the loop-shaping performance weighting function.

From the standard assumption for optimal H_∞ control [12], the derived controller requires a condition $D_{21}(k)D_{21}^T(k) \succ 0$ for all k . Unfortunately, the typical approach to enforce multi-rate sampling and actuation [14] will not work here because this would result in $D_{21}(k)D_{21}^T(k)$ being singular. In this paper, we consider the block diagram shown in Fig. 7 for the multi-rate optimal H_∞ control synthesis. Here, we introduce a fictitious disturbance input w_2 which will be injected into the feedback signal y when the PES is unavailable so that the non-singularity assumption of $D_{21}(k)D_{21}^T(k)$ can be attained. Notice that if the gain of the resulting time varying controller K is zero when the PES measurement is unavailable at the time of k , then this fictitious noise will not affect the minimum closed-loop induced norm and

the resulting optimal H_∞ controller. This expectation is achieved when the minimum entropy H_∞ control synthesis technique proposed in this paper is used, as will be discussed in detail later.

Unlike the standard H_∞ control problem formulation [17], the performance weighting function here is moved to the disturbance input side. By doing so, the feedback signal y is affected by a ‘‘colored’’ disturbance ($W_p w_1$) more directly when the sampling rate is lower than the actuation rate. In order to maintain the same H_∞ constraints as those that were used in Section 4.1, it is necessary to use the control synthesis architecture shown in Fig. 7, where the weighting functions W_p and W_Δ are the same as the weighting functions in Section 4.1.

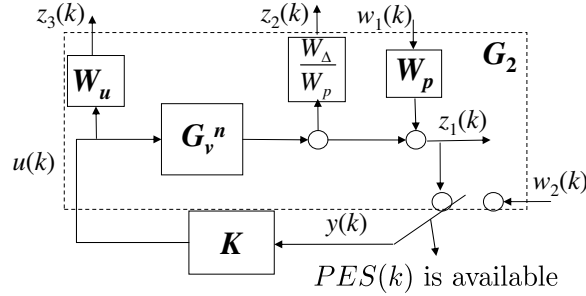


Figure 7: Control design formulation for HDDs with multi-rate sampling and actuation

As a result, we can formulate the optimal H_∞ control design problem in (4) by replacing the system G by G_2 , where G_2 is indicated by the dashed box in Fig. 7. Thus, G_2 is the open-loop map from $\begin{bmatrix} w_1 & w_2 & u \end{bmatrix}^T$ to $\begin{bmatrix} z_1 & z_2 & z_3 & y \end{bmatrix}^T$, which can be represented by the following LPTV system with period $N = 3$:

$$G_2 \sim \begin{bmatrix} x(k+1) \\ z(k) \\ y(k) \end{bmatrix} = \begin{bmatrix} A & B_1 & B_2 \\ C_1 & D_{11} & D_{12} \\ C_2(k) & D_{21}(k) & 0 \end{bmatrix} \begin{bmatrix} x(k) \\ w(k) \\ u(k) \end{bmatrix} \quad (16)$$

where

$$\begin{bmatrix} C_2(k) & D_{21}(k) \end{bmatrix} = \begin{cases} \begin{bmatrix} C_{2m} & \begin{bmatrix} D_{21m} & 0 \end{bmatrix} \\ 0 & \begin{bmatrix} 0 & 1 \end{bmatrix} \end{bmatrix} & \text{PES is unavailable} \\ \begin{bmatrix} 0 & \begin{bmatrix} 0 & 1 \end{bmatrix} \end{bmatrix} & \text{otherwise} \end{cases} \quad (17)$$

Notice that all the matrices (16) are constants except $C_2(k)$ and $D_{21}(k)$. Since all the matrices involved in the computation of the state feedback Riccati equation solution (6) in Step 1) are constant, the solution $X(k)$ will converge to a constant matrix which can be computed via its corresponding discrete algebraic Riccati equation (DARE). Moreover, the parameters X , T and F that are computed in Step 1-3) are constant, which implies the parameters $\bar{A}(k)$ and $T_{22}^{-1}(k)\bar{C}_{12}(k)$ in the proposed controller (5) will also be constant. Additionally, the filtering Riccati equation solution $Y(k)$, which is computed forwards in time using (8) and a zero initial condition, will converge to a steady-state periodic solution with period N , as demonstrated by Lemma 1. It turns out that the filter gains $F_t(k)$ and $L_t(k)$ will also be periodic with period N . It can also be shown [12] that both $\tilde{T}_{12}(k)$ and $\tilde{F}_2(k)$ are equal to zero at the instance k

Table 1: Simulation results for single and multi rate control designs

| | 3 σ PES (% of track) | |
|--------------------|-----------------------------|-------|
| | Nominal | Worst |
| Single-rate design | 10.7 | 11.4 |
| Multi-rate design | 9.2 | 9.6 |

when the PES is unavailable. Thus, both $F_t(k)$ and $L_t(k)$ are also equal to zero at these instances, justifying the use of the fictitious disturbance w_2 in the control synthesis methodology. As a result, the minimum closed-loop ℓ_2 induced norm and the optimal H_∞ controller are unaffected by the use of the fictitious disturbance w_2 in the control synthesis. With the zero gains of $F_t(k)$ and $L_t(k)$ at the instance when the PES is unavailable, the time varying control parameter $\bar{C}_2(k) = C_2(k) + D_{21}(k)F_1$ in (5) can be simply replaced by the constant parameter $\bar{C}_{2m} = C_{2m} + \begin{bmatrix} D_{21m} & 0 \end{bmatrix} F_1$ without changing the controller. As a result, for the HDD servo systems with multi-rate sampling and actuation, all of the control parameters of the minimum entropy H_∞ controller shown in (5) are constant except $F_t(k)$ and $L_t(k)$.

Performing a multi-rate optimal H_∞ control synthesis described above, produces a multi-rate H_∞ controller that returns the minimum ℓ_2 induced norm of $\gamma^* = 1.0$.

With the more aggressive performance weighting function shown in Fig. 4, the obtained optimal ℓ_2 induced norm of $\gamma^* = 1.0$ implies that the multi-rate strategy has the ability to improve the control performance. In order to further highlight the performance and robustness improvement that can be attained by the presented control synthesis algorithm for a higher actuation rate, a time domain simulation study was performed using both the single-rate optimal H_∞ control designed in Section 4.1 and the multi-rate optimal H_∞ control designed in this subsection. To evaluate the robust performance of the two control designs, each controller was tested on 50 different plants, which were randomly generated from (12) with the uncertainty weighting function in (14) by using Matlab function “`usample`”. Note that the disturbance models for our time domain simulation are provided in [13].

Table 1 contains the root mean square (RMS) 3σ values of the PES for the nominal plant and the worst-case results for each controller. These results indicate that a controller with a higher actuation rate is able to not only reduce the 3σ PES by 14.0% for the nominal plant, but also improve the servo performance for the worst-case situation by 15.8%.

5 Experimental study

In order to further evaluate our proposed optimal H_∞ control synthesis methodology, we used the proposed algorithm to design a controller and then implemented the resulting controller on a real hard disk drive with missing PES samples. The tested hard disk drive was provided by Western Digital Corporation. For this 3.5” disk drive, the number of servo sectors is 256 and the spindle rotation speed is 7200 RPM. The servo patterns on some servo sectors at the inside

diameter (ID) are inaccessible for the servo system to generate PES. Specifically, we found that PES is unavailable on the following 51 servo sectors:

$$M_{\text{miss}} = \{0, 4, 8, 17, 21, 25, 34, 38, 42, 47, 51, 55, 59, 64, 68, 72, 81, 85, 89, 98, 102, 106, 111, 115, 119, 123, 128, 132, 136, 145, 149, 153, 162, 166, 170, 179, 183, 187, 192, 196, 200, 209, 213, 217, 226, 230, 234, 239, 243, 247, 251\}.$$

Such a HDD servo with missing PES samples can be still represented as the block diagram in Fig. 6 and we also consider the block diagram shown in Fig. 7 for the optimal H_∞ control synthesis [2]. Then, the system shown in (16) has a large period, i.e. $N = 256$.

As presented in [2], the nominal VCM model $G_v^n(s)$ was identified to match the experiment frequency response which was measured on the disk area where there are no missing PES samples. Note that in order to reduce the control order, the nominal VCM plant was identified as an 8th order model. In addition, the weighting functions for the control design formulation in Fig. 7 were determined as

$$W_\Delta(z) = \frac{0.985z - 0.693}{z + 0.041}$$

$$W_p(z) = \frac{0.156z^5 - 0.666z^4 + 1.14z^3 - 0.968z^2 + 0.41z - 0.07}{z^5 - 4.933z^4 + 9.739z^3 - 9.617z^2 + 4.75z - 0.939}$$

$$W_u = 4.$$

As a result, the VCM plant could have an unstructured uncertainty producing a $\pm 28\%$ gain variation at low frequency and a $\pm 175\%$ gain variation at high frequency with the chosen W_Δ , while the frequency response of W_p^{-1} associated with disturbance attenuation is shown in Fig. 9.

After applying our developed control algorithm, an optimal ℓ_2 induced norm of $\gamma^* = 0.91$ was obtained. We used balanced truncation [18] to reduce the order of the resulting controller from 19 to 12. This allowed us to implement the controller on the disk drive's own processor by changing the firmware code. In addition, since control parameters $F_t(k)$ and $L_t(k)$ in (5) are time-varying, we have to reduce the number of these control parameters for their implementation on real HDDs. As demonstrated in [2], the non-zero time-varying parameters $F_t(k)$ and $L_t(k)$ have very small variations, which motivates us to approximate these time-varying control parameter values using their average values over M_{miss} .

the desired disturbance attenuation.

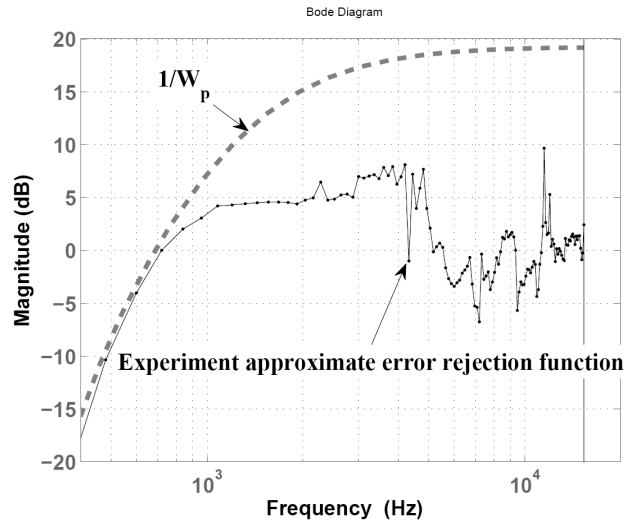


Figure 9: Experiment result for the experimental approximate error rejection function

6 Conclusion

The optimal H_∞ control synthesis via discrete Riccati equations for general discrete-time linear periodically time-varying systems was studied in this paper. Using the results in [10], we first developed the optimal H_∞ control synthesis algorithm for general discrete-time linear time-varying systems. The control synthesis algorithm was subsequently applied to LPTV systems, and it was verified that the resulting controllers are also periodically time-varying. The presented control synthesis technique was evaluated by designing both single-rate and multi-rate optimal H_∞ track-following controllers for HDDs. In the case of single-rate control, the optimal H_∞ controller designed using the proposed synthesis technique was compared to the one designed using the Matlab function ‘hinfsyn’. Simulation results suggested that the former technique is more numerically robust in calculating optimal discrete-time H_∞ controllers for discrete-time linear time-invariant systems than the latter. Simulation results further demonstrated the presented control synthesis algorithm is also applicable to HDD servos with multi-rate sampling and actuation, while the ‘hinfsyn’ function in Matlab is only applicable for LTI plants. Moreover, an experimental study, which consisted of implementing the developed control algorithm on a real disk drive with missing PES sampling data, demonstrated its effectiveness in handling LPTV systems with a large period and attaining desirable disturbance attenuation.

Acknowledgment

The authors would like to thank Western Digital Corporation for providing invaluable information to perform this study. This work was performed with the support of the UC Berkeley Computer Mechanics Laboratory (CML) and a research grant from Western Digital Corporation.

References

- [1] M. Gei, S. Roccabianca, and M. Bacca, “Controlling bandgap in electroactive polymer-based structures,” *IEEE/ASME Trans. on Mechatronics*, vol. 16, no. 1, pp. 102–107, 2011.
- [2] J. Nie, E. Sheh, and R. Horowitz, “Optimal H_∞ Control For Hard Disk Drives With An Irregular Sampling Rate,” *to appear in Proc. of the 2011 American Control Conference*, San Francisco, CA.
- [3] R. Conway and R. Horowitz, “Guaranteed Cost Control for Linear Periodically Time-Varying Systems with Structured Uncertainty and a Generalized H_2 Objective,” *Mechatronics*, vol. 20, no. 1, pp. 12–19, 2010.
- [4] K. Kalyanam and T. Tsao, “Experimental study of adaptive-Q control for disk drive track-following servo problem,” *IEEE/ASME Trans. on Mechatronics*, vol. 15, no. 3, pp. 480–491, 2010.
- [5] K. Chan, W. Liao, and I. Shen, “Precision positioning of hard disk drives using piezoelectric actuators with passive damping,” *IEEE/ASME Trans. on Mechatronics*, vol. 13, no. 1, pp. 147–151, 2008.
- [6] A. Iqbal, Z. Wu, and F. Ben Amara, “Mixed-sensitivity H_∞ control of magnetic-fluid-deformable mirrors,” *IEEE/ASME Trans. on Mechatronics*, vol. 15, no. 4, pp. 548–556, 2010.
- [7] G. Zames, “Feedback and optimal sensitivity: Model reference transformations multiplicative seminorms, and approximate inverses,” *IEEE Trans. on Automatic Control*, vol. 26, no. 2, pp 301–320, 1981.
- [8] J. Doyle, K. Glover, P. Khargonekar, and B. Francis, “State-Space Solutions to Standard H_2 and H_∞ Control Problems,” *IEEE Trans. on Automatic Control*, vol. 34, no. 8, pp. 831–847, 1989.
- [9] P. Iglesias and K. Glover, “State-space approach to discrete-time control,” *International Journal of Control*, vol. 54, no. 5, pp. 1031–1073, 1991.
- [10] M. A. Peters and P. A. Iglesias, *Minimum Entropy Control for Time-Varying Systems. Systems & Control: Foundations & Applications*, Birkhäuser, Boston, MA, 1997.
- [11] R. Conway and R. Horowitz, “Analysis of H_2 Guaranteed Cost Performance,” *Proceedings of the 2009 Dynamic Systems and Control Conference*, Hollywood, California, 2009.

- [12] J. Nie, "Control Design and Implementation of Hard Disk Drives," PhD Thesis, University of California, Berkeley, CA, 2011.
- [13] IEEJapan technical committee on Nano-Scale Servo (NSS) system. NSS homepage, 2006. URL <http://mizugaki.iis.u-tokyo.ac.jp/nss/>.
- [14] R. Nagamune, X. Huang, and R. Horowitz, "Multi-rate track-following control with robust stability for a dual-stage multi-sensing servo systems in HDDs," *Proceedings of the Joint 44th IEEE Conference on Decision and Control and European Control Conference*, pp.3886-3891, 2005.
- [15] L. Yang and M. Tomizuka, "Short seeking by multirate digital controllers for computation saving with initial value adjustment," *IEEE/ASME Trans. on Mechatronics*, vol. 11, no. 1, pp 9–16, 2006.
- [16] J. Nie and R. Horowitz, "Design and Implementation of Dual-Stage Track-Following Control for Hard Disk Drives", *Proceedings of the Dynamic Systems and Control Conference*, Hollywood, California, 2009.
- [17] S. Skogestad and I. Postlethwaite, *Multivariable feedback control: analysis and design*, John Wiley, Hoboken, NJ, 2005.
- [18] B. Moore, "Principal Component Analysis in Linear Systems: Controllability, Observability, and Model Reduction," *IEEE Trans. on Automatic Control*, vol. 26, no. 1, pp 17–31, 1981.